Chemical Geology 397 (2015) 106–117

Contents lists available at ScienceDirect

Chemical Geology

journal homepage: www.elsevier.com/locate/chemgeo

The Mg/Ca–temperature relationship in brachiopod shells: Calibrating a potential palaeoseasonality proxy

Scott Butler [a,b], Trevor R. Bailey [b,*], Caroline H. Lear [a], Gordon B. Curry [c], Lesley Cherns [a], Iain McDonald [a]

[a] School of Earth and Ocean Sciences, Cardiff University, Park Place, Cardiff CF10 3AT, UK
[b] Department of Natural Sciences, Amgueddfa Cymru, National Museum Wales, Cathays Park, Cardiff CF10 3NP, UK
[c] School of Geographical and Earth Sciences, University of Glasgow, Gregory Building, Lilybank Gardens, Glasgow G12 8QQ, UK

ARTICLE INFO

Article history:
Received 19 August 2014
Received in revised form 15 January 2015
Accepted 18 January 2015
Available online 26 January 2015

Editor: Michael E. Böttcher

Keywords:
Brachiopod
Temperature
Seasonality

ABSTRACT

Brachiopods are long-lived, long-ranging, extant organisms, of which some groups precipitate a relatively diagenetically stable low magnesium calcite shell. Previous work has suggested that the incorporation of Mg into brachiopod calcite may be controlled by temperature (Brand et al., 2013). Here we build upon this work by using laser ablation sampling to define the intra-shell variations in two modern brachiopod species, *Terebratulina retusa* (Linnaeus, 1758) and *Liothyrella neozelanica* (Thomson, 1918). We studied three *T. retusa* shells collected live from the Firth of Lorne, Scotland, which witnessed annual temperature variations on the order of 7 °C, in addition to four *L. neozelanica* shells, which were dredged from a water depth transect (168–1488 m) off the north coast of New Zealand. The comparison of intra-shell Mg/Ca profiles with shell $\delta^{18}O$ confirms a temperature control on brachiopod Mg/Ca and supports the use of brachiopod Mg/Ca as a palaeoseasonality indicator. Our preliminary temperature calibrations are $Mg/Ca = 1.76 \pm 0.27\ e^{(0.16 \pm 0.03)T}$, $R^2 = 0.75$, for *T. retusa* and $Mg/Ca = 0.49 \pm 1.27\ e^{(0.2 \pm 0.11)T}$, $R^2 = 0.32$, for *L. neozelanica* (errors are 95% confidence intervals).

1. Introduction

Magnesium to calcium ratios (Mg/Ca) have been established as proxies for marine temperatures in a range of calcite shells, e.g., benthic and planktonic foraminifera and ostracodes (Chivas et al., 1986; Dwyer et al., 1995; Nürnberg et al., 1996; Rosenthal et al., 1997). Although the Mg/Ca–temperature relationship in biogenic carbonates likely represents a combination of thermodynamic and physiological effects (Rosenthal et al., 1997), initial studies by Lee et al. (2004), Perez-Huerta et al. (2008) and Brand et al. (2013) suggest that a consistent Mg/Ca–temperature dependence may also be found in brachiopod calcite.

As a tool for obtaining palaeoclimate data rhynchonelliform brachiopods have several benefits when compared to other fauna recording palaeoclimate signals. All shells of the subphylum Rhynchonelliformea have a fibrous secondary layer of low magnesium calcite (Williams et al., 1996), which is the most diagenetically stable form of $CaCO_3$ (e.g., Lowenstam, 1961; Veizer et al., 1986). Rhynchonelliform brachiopod shells are present from the Early Cambrian to the present (Zhang et al., 2008). This long fossil record offers the potential to collect palaeoclimate data as far back as the early Palaeozoic and to calibrate fossil data against modern observations. Excluding the pelagic larval stage, brachiopods stay in one place on the ocean floor throughout their life and are therefore static recorders of their environment. Brachiopod shells also have distinct growth lines. Although poorly understood, these possibly represent seasonal change (Buening and Carlson, 1992) and may also form biannually at times of physiological and environmental stress, such as spawning (Curry, 1982). Therefore, brachiopods may represent an untapped archive of past seasonality.

A recent study of Mg in rhynchonelliform brachiopod shells using synchrotron X-ray absorption near edge spectroscopy has confirmed that Mg resides within the calcite lattice and is therefore suitable for use as a temperature proxy (Cusack et al., 2008). Modern rhynchonelliform brachiopod shells all have an outer primary layer of prismatic calcite and an inner secondary layer of fibrous calcite, and some species have an additional tertiary layer of prismatic calcite (Williams and Cusack, 2007). Previous laser ablation studies of rhynchonelliform brachiopods using spot analyses have shown that the primary layer displays high and variable Mg concentrations (Perez-Huerta et al., 2008). Mg concentrations within the secondary layer however are reproducible (Perez-Huerta et al., 2008) and symmetrical in transects perpendicular to the main axis of growth (Lee et al., 2004). Both these studies suggest that secondary layer calcite might record seawater temperature signals. In addition, it has been shown that secondary layer calcite is precipitated in oxygen isotopic equilibrium with the ambient seawater, when sampling has avoided

* Corresponding author.
E-mail address: Trevor.Bailey@museumwales.ac.uk (T.R. Bailey).

http://dx.doi.org/10.1016/j.chemgeo.2015.01.009

shell parts subject to resorption and renewed calcification during life (the muscle scars, loop and teeth) (Parkinson et al., 2005; Yamamoto et al., 2010a, 2010b, 2011; Brand et al., 2014).

A study of the Recent rhynchonelliform, *Laqueus rubellus*, demonstrated that Mg/Ca maxima coincide with seasonal periods of shell growth evidenced by the morpho-statistical approach of calculating deviations from a spiral shell growth curve (Pérez-Huerta et al., 2014). Therefore, we aim to test the hypothesis that the cyclic variations in intra-shell Mg/Ca profiles represent seasonal temperature variations. We first describe a laser ablation method that retrieves profiles of trace element to calcium ratios from brachiopod shells that are reproducible on the sub-mm scale. We then compare laser trace element and microdrilled stable isotope data to determine whether seasonal temperature variations are recorded in Mg/Ca profiles of modern shells of *Terebratulina retusa* (Linnaeus [Linné], 1758) and *Liothyrella neozelanica* (Thomson, 1918). In addition, we assess the mean shell Mg/Ca of modern *L. neozelanica* specimens from a water depth transect. Our combined approach enables us to present an estimated sensitivity of brachiopod Mg/Ca to temperature.

2. Brachiopod specimens

The modern species *T. retusa* has a recorded depth range of 18–2157 m and is patchily distributed around the central and eastern North Atlantic as far north as the Barents Sea and as far south as Cape Verde, and it is also present in the Mediterranean (Logan, 2007). Shells 1 to 3 are three *T. retusa* collected alive from a large population dredged from a 150 to 200 m deep depression in the Firth of Lorne, Scotland (56°26′N, 5°38′W, Fig. 1), where they are predominantly attached to a substrate of horse mussels (*Modiolus modiolus*) (Curry, 1982). This locality has water temperatures ranging from 6.5 to 13 °C throughout the year (Curry, 1982) and a $\delta^{18}O$ of 0.06 ‰ VSMOW (Parkinson et al., 2005). Ten salinity measurements taken between February 1982 and

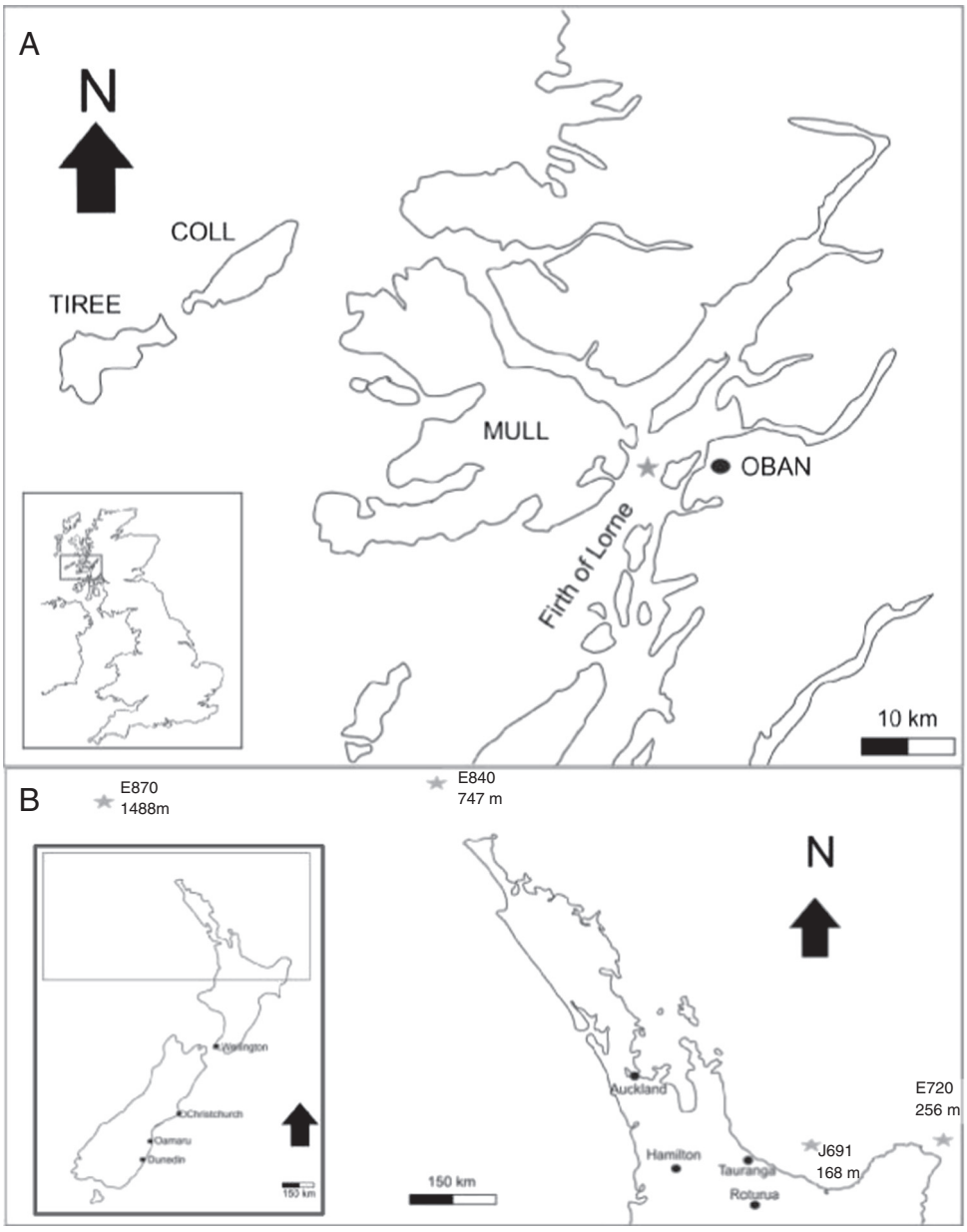

Fig. 1. Maps of the United Kingdom and New Zealand with brachiopod collection sites marked by stars.

February 1983 from 120 to 200 m depth from three sites within 10 km of the sampling site (Grantham, 1983; Grantham et al., 1983a, 1983b) showed no significant seasonal variation, having a February average of 33.8 ± 0.2 practical salinity units (1sd, $n = 6$) and a July average of 33.7 ± 0.1 psu (1sd, $n = 4$).

L. neozelanica is recorded from waters around New Zealand as well as the Chatham Rise (Logan, 2007). Specimens J691, E720, E840 and E870 were kindly donated from the Invertebrate Collection of the National Institute of Water and Atmospheric Research (NIWA), Wellington, New Zealand. Valves were recovered by trawling and dredging between 1962 and 1989, from water depths between 168 m and 1488 m from locations north of North Island within the East Auckland Current (Fig. 1), and were subsequently stored dry. Corresponding temperature and salinity data from single CTD casts near these locations vary between 3 and 15 °C and between 34.6 and 35.4 psu (WOCE, 2002) (Table 1).

The shell of *L. neozelanica* differs from that of *T. retusa*, by having an additional layer. The bulk of the valve thickness is composed of this tertiary layer prismatic calcite, which is precipitated closest to the interior margin of the shell.

3. Methods

3.1. Preparation of Shells

The valves were manually separated where necessary, cleaned using deionised water and a fine brush, and set in a polyester resin with a methyl ethyl ketone peroxide catalyst. Valves were sectioned, following the schematic in Fig. 2, with a diamond wafering saw and lapped with silicon carbide. For each species, one valve was sectioned longitudinally to investigate ontogenetic effects, and the remainder were sectioned transversely ~5 mm from the anterior margin to avoid potential crystallographic effects present in the posterior region (Perez-Huerta et al., 2011). The theoretical Mg/Ca profiles (Fig. 2) are drawn assuming continuous shell growth throughout the year and that shell Mg/Ca directly reflects annual variations in seawater temperature. The growth pattern of the brachiopod shell thus predicts a symmetrical profile in the transverse sections, which would provide a useful additional constraint when assessing the robustness of measured profiles, particularly for fossil specimens.

3.2. Analysis by laser ablation ICP-MS

The sectioned shells were sampled using a New Wave Research 213 nm laser ablation system, coupled to a Thermo X Series2 Inductively Coupled Plasma Mass Spectrometer (LA-ICP-MS) at Cardiff University using the parameters shown in Table 2. The sample was moved under the laser at 11 μm/s. At higher speeds, fragments of shell were seen to break off, causing undesired spikes in signal intensity on ionisation. At slower laser speeds, signal intensity was attenuated as less material escaped the deeper laser ablation pits. Laser tracks were run as close to the inside of the shell as possible to stay within the secondary layer for *T. retusa*, and within the tertiary layer for *L. neozelanica*. Laser tracks were curved so that the laser remained at the same distance from the inner margin of the shell.

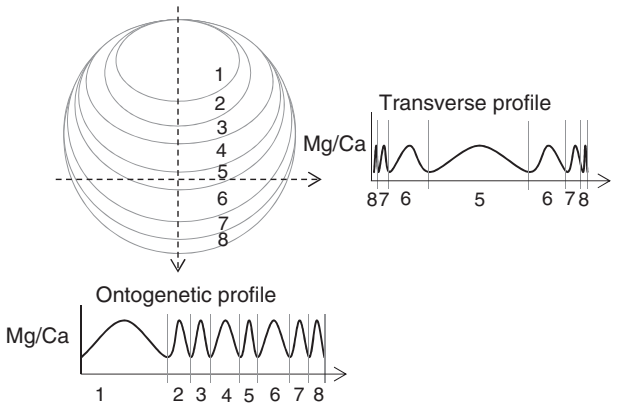

Fig. 2. Schematic showing theoretical Mg/Ca profiles from the two different directions of sectioning, drawn assuming continuous shell growth and that shell Mg/Ca directly reflects annual variations in seawater temperature over a period of 8 years.

^{24}Mg, ^{25}Mg, ^{27}Al, ^{43}Ca, ^{44}Ca, ^{48}Ca, ^{55}Mn, ^{57}Fe, ^{84}Sr, ^{86}Sr and ^{88}Sr peaks were averaged by the mass spectrometer every 0.5 s. The isotope ^{25}Mg was used as it gives more reproducible results than ^{24}Mg, possibly due to interference of doubly charged ^{48}Ca on mass 24. ^{86}Sr was chosen over ^{88}Sr to avoid overloading the detector at higher signal levels. NIST 610 glass was analysed as a standard between each sample track, as similar concentrations of Mg are found within modern brachiopod shells and this glass (466 μg/g, Pearce et al., 1997). Standards were measured about every 7 min and show a high level of reproducibility throughout each day of analysis <8 %RSD for ^{25}Mg/^{43}Ca, and <4%RSD for ^{86}Sr/^{43}Ca and ^{43}Ca/^{48}Ca.

Each individual data point represents an averaged signal from material ablated by a 40 μm laser spot that moved 5.5 μm along the laser track; the spatial resolution is therefore ~50 μm. Valve profiles were constructed from several individual tracks subsequently stitched together. Due to a 5 s time delay between firing the laser and obtaining a stable signal, adjoining tracks were overlapped by 60 μm to ensure continuous data profiles across the shell. This overlap meant that for a new track, the first 11 data points after the gas blank were omitted from the results as they were obtained from the previously ablated track. The total analysis time for a 30 mm traverse was about 2.5 hours.

3.3. Screening of laser data

High Mg/Ca and Sr/Ca signals were occasionally recorded at the valve margins, which resulted from the ablation of resin. These data were easily identified by their reduced ^{43}Ca signal intensity and removed from the profiles presented here. Alongside Mg, Sr and Ca, the isotopes ^{27}Al, ^{55}Mn and ^{57}Fe were collected for the purpose of screening for contamination of the brachiopod calcite. Diagenetic alteration of original shell chemistry can cause incorporation of Fe and Mn in the crystal lattice, while selectively removing Sr, and can change original Mg concentrations in either direction depending on the circumstances (Brand and Veizer, 1980, Brand, 2004). Aluminium was measured as an indicator of contamination by clay minerals, which can cause elevated Mg/Ca values (Barker et al., 2003).

Table 1
L. neozelanica valves from the north coast of North Island, New Zealand.

Shell ID	Date collected	Latitude/longitude	Depth of recovery (m)	Temperature at depth of recovery from closest CTD cast (°C)	Section
J691	09/09/1974	−37.5583000183/176.9799957275	168	15.0	Transverse
E720	24/03/1967	−37.5499992371/178.5832977295	256	13.5	Transverse and ontogenetic section
E840	16/03/1968	−33.8666992188/172.2666931152	757	7.5	Transverse
E870	20/03/1968	−34.0833015442/168.1667022705	1488	3.0	Transverse

Table 2
Laser parameters for LA-ICP-MS analysis.

Laser model	New wave research UP213 UV
Energy density (fluence)	3.0 Jcm^{-2}
Focus	Fixed at surface
Repetition rate	10 Hz
Track width	~40 μm
Acquisition mode	Time resolved analysis
Duration of gas blank	35 s

As the *T. retusa* shells in this study are modern and were collected alive, the effects of post-mortem diagenesis are absent. The data in this study represent the natural levels of incorporation of elements into the shell before death. In contrast, the dredged *L. neozelanica* samples each experienced variable unknown lengths of time on the sea-floor after death. As a result, two of these shells (E840 and E870) have sub-mm scale borings infilled by sediment. Such 'contaminated' areas of the element profiles were identified by elevated Al/Ca (up to 1800 μmol/mol), which correlated with elevated Mg/Ca (up to 200 mmol/mol). Data with Al/Ca > 4 μmol/mol were therefore discarded from the *L. neozelanica* profiles.

3.4. Stable isotope analysis

Powder for stable isotope analyses was drilled using a New Wave Research Micromill after acquisition of LA-ICP-MS data, in the same location as the ablated tracks. Drilled trenches were of lengths of 500–1200 μm, depths of 100–200 μm, and widths of ~60 μm. Trenches with smaller dimensions did not produce enough powder for accurate stable isotope analysis. After each trench was drilled and the powdered sample transferred to a glass vial, the trench, sample surface and drill bit were cleaned with deionised water and a brush to ensure no cross contamination between trenches. Trenches were drilled as close to the inner margin of the shell as possible, as only the inner half to two-thirds of the shell thickness are known to be in oxygen isotopic equilibrium with the ambient sea water (Auclair et al., 2003; Parkinson et al., 2005). Samples were analysed at Cardiff University using an automated carbonate preparation device (Kiel-III) coupled online to a Thermo Finnigan MAT252 stable isotope mass spectrometer. Analytical precision was determined by repeated measurements of in house (Carrara Marble) and international (NBS19) carbonate standards with a precision of 0.06‰. All results are reported relative to the PDB scale.

4. Results

4.1. Reproducibility of intra-shell element/calcium profiles

To assess the reproducibility of LA-ICP-MS intra-shell profiles, we ran repeat analyses on two different short tracks from the dorsal valve of *T. retusa* shell 1 (see inset, Fig. 3). Identical elemental profiles are not expected as subsequent traverses sample slightly deeper in the valve on each run. However, Mg/Ca profiles of repeated tracks have reassuringly similar shaped profiles and Mg/Ca ranges (Fig. 3). Furthermore, the Mg/Ca values of a run are positively correlated with subsequent runs, with R^2 values between 0.70 and 0.81. Where the Mg/Ca of Track 1 reaches > 20 mmol/mol at ~0.3 mm, it is likely that the laser began sampling material from the primary layer. Mg/Ca values are closely comparable to the data of Perez-Huerta et al. (2008) who produced profiles using five laser spots across the width of *T. retusa* valves from the same locality. Three

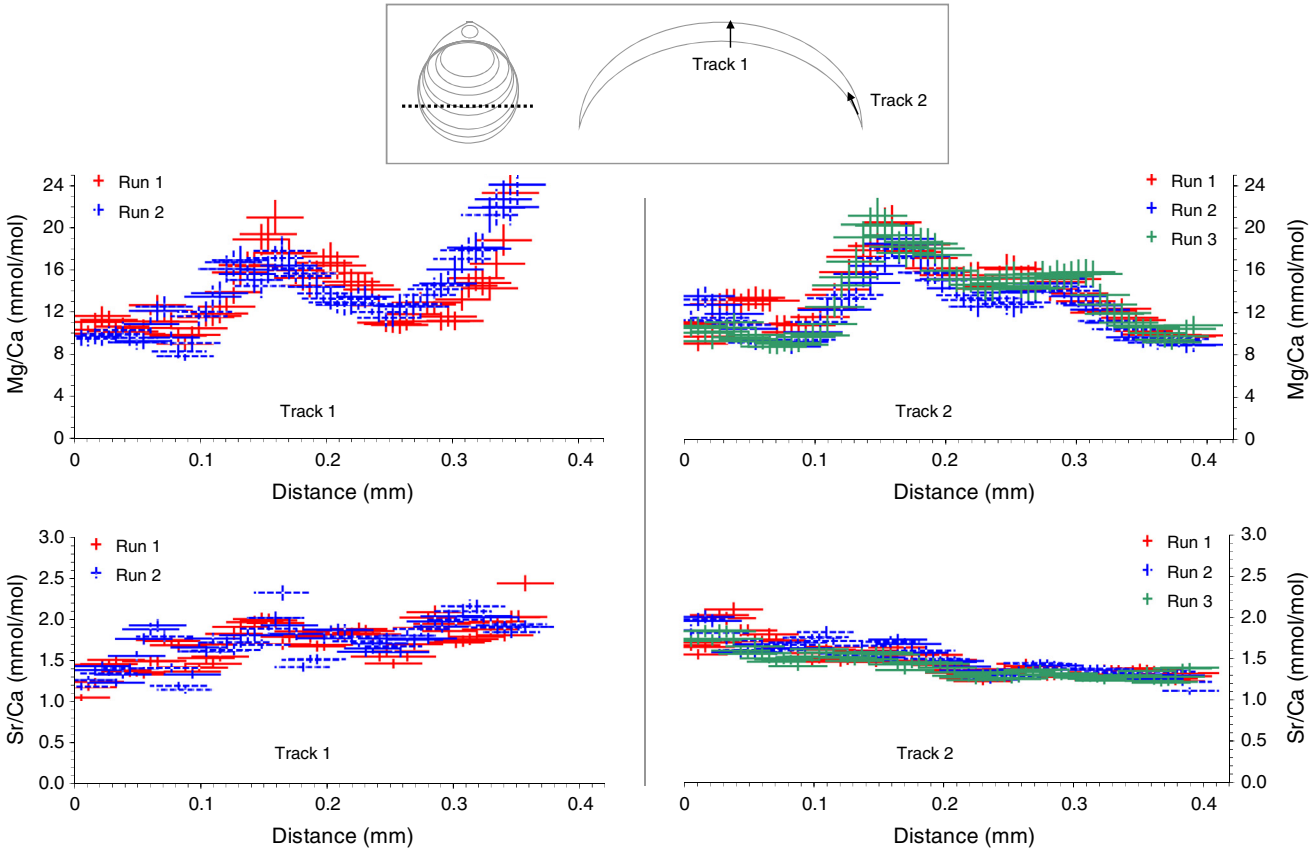

Fig. 3. Repeat Mg/Ca and Sr/Ca profiles from *T. retusa* dorsal valve 1D: Track 1, across the sectioned valve from interior to exterior margin, Track 2, in the middle of the sectioned valve parallel to the interior margin. The *x* error bars reflect the spatial resolution of the sampling, and the *y* error bars reflect analytical uncertainty based on standards run throughout the day (8% RSD for Mg/Ca and 4% RSD for Sr/Ca). For this and all subsequent figures, the dashed line in the inset box indicates the approximate line of section, and the arrowed lines show the position of the laser tracks.

repeated runs of Track 2, parallel to the inner margin of the valve, also yield consistent Mg/Ca profiles with ranges of 13.5 ± 1.5 mmol/mol (Fig. 3).

Repeated Sr/Ca profiles are also consistent in shape and Sr/Ca range, although the Sr/Ca values of a run and subsequent runs are more weakly correlated (R^2 between 0.35 and 0.72) than is the case for Mg/Ca. Both runs of track 1 have a Sr/Ca range of ~1.4 mmol/mol. The repeated runs of Track 2 have a Sr/Ca range of 0.9 ± 0.1 mmol/mol. Mg/Ca and Sr/Ca do not co-vary in Track 2, parallel to the shell margin, although appear to be weakly correlated in Track 1, across the shell width (R^2 of 0.41 and 0.55), which includes both the primary and secondary calcite layers (Fig. 3).

4.2. Geochemical variability along an ontogenetic section of T. retusa

Element profiles were taken from the posterior to the anterior margin of the ventral valve of *T. retusa* shell 1 (1 V, Fig. 4) to examine variations in shell chemistry from the juvenile to adult portions of the valve. The full range of Mg/Ca variation in valve 1 V reaches up to 120 mmol/mol in the youngest shell material, an enrichment of ~10 times the average value of the adult shell (Fig. 4, 1V inset). Including this large peak, the Mg/Ca profile of 1 V shows 9 pairs of Mg/Ca peaks and troughs spaced ~2–3 mm apart, with all except the youngest two being between 6 and 12 mmol/mol in peak-to-trough magnitude (Fig. 4).

To allow the comparison of $\delta^{18}O$ and Mg/Ca data on the same spatial scale, we plot laser Mg/Ca data averaged over the same distances as the trenches drilled for $\delta^{18}O$ analysis ('Averaged Mg/Ca'). In the youngest part of valve 1 V, the profiles of $\delta^{18}O$ and averaged Mg/Ca do not co-vary (0–7.5 mm from the posterior edge of the valve, shaded grey). However, Mg/Ca maxima and minima correspond with lighter and heavier $\delta^{18}O$ respectively, from 7.5 mm onwards, the adult portion of the valve.

The ontogenetic Sr/Ca profile (1 V) displays values as high as 2.8 mmol/mol at 0–1.2 mm, which is around twice the average value of the rest of the valve. Between 2 and 15 mm, Sr/Ca show fluctuations with peak-to-trough magnitudes of up to 0.5 mmol/mol. Sr/Ca maxima generally correspond to Mg/Ca maxima; however, Sr/Ca variations are more poorly defined than the Mg/Ca peaks and troughs.

Laser $^{43}Ca/^{48}Ca$ profiles are included as a monitor of instrument performance and an indicator of the possible inclusion of non-carbonate material in the shell. There is no significant variation in this ratio on profile 1 V except for a small increase in scatter centred around 1 mm.

4.3. Geochemical variability along a transverse section of T. retusa

Profile 1D of Fig. 4 reports data obtained from a transverse section of the dorsal valve of shell 1. This section was cut at approximately two-thirds of the distance from the shell posterior margin to avoid potential crystallographic effects present in the posterior region (Perez-Huerta

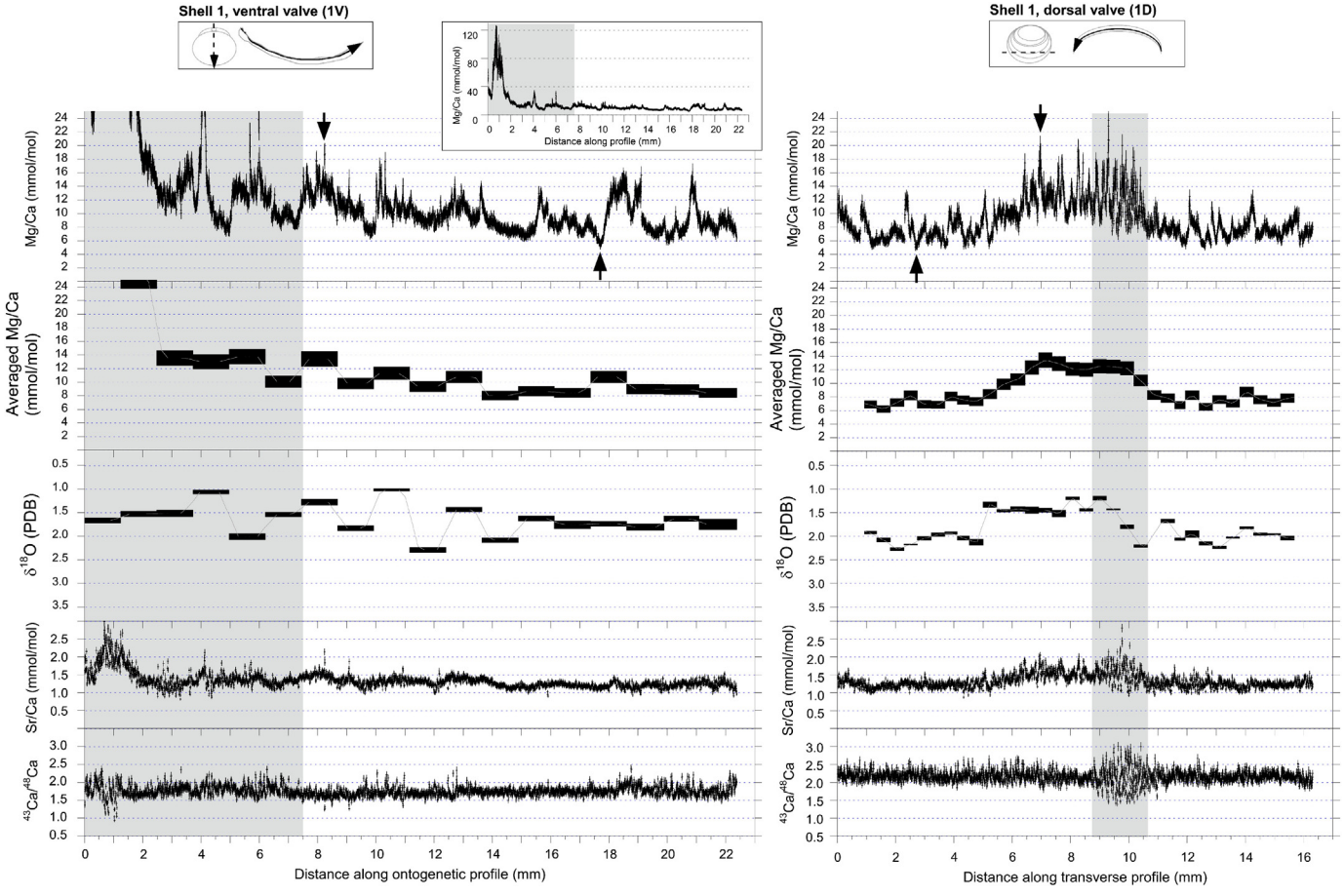

Fig. 4. Profiles of laser Mg/Ca, Sr/Ca and $^{43}Ca/^{48}Ca$ intensity data, and microdrilled $\delta^{18}O$ data from *T. retusa* shell 1. 'Averaged Mg/Ca' is a plot of the laser Mg/Ca data averaged over the same distances as the trenches drilled for $\delta^{18}O$ analysis. 1 V is an ontogenetic section, from the posterior to anterior margin of the ventral valve. The inset box shows the full range of Mg/Ca values, and grey shading denotes where $\delta^{18}O$ and averaged Mg/Ca do not co-vary. 1D is a transverse section, the grey shading denotes a portion removed through data screening due to the coincidence of high Mg/Ca and Sr/Ca with scattered $^{43}Ca/^{48}Ca$. The maximum and minimum values of the adult portions of the laser Mg/Ca profiles are indicated by arrows. For laser data, *y* error bars reflect analytical uncertainty based on standards run throughout the day (±8% RSD for Mg/Ca, and ±4% RSD for Sr/Ca and $^{43}Ca/^{48}Ca$). For $\delta^{18}O$, the *y* error bars represent ±1 SD of the individual measurements. (For interpretation of the references to colour in this figure, the reader is referred to the web version of this article.)

et al., 2011), and to allow comparison between ventral (1 V) and dorsal (1D) valves of the same shell.

The $^{43}Ca/^{48}Ca$ ratio is constant at 2.2 ± 0.4 across this transverse profile, except for a short portion with more variable ratios (9–10.5 mm), which correspond to elevated Mg/Ca and Sr/Ca values (1D, Fig. 4, shaded grey). The cause of this increased scatter is unknown but is likely to be either contamination by clay minerals, non-shell carbonate or resin causing isobaric interference in the Ca mass range. These shaded data are not considered in further discussion, although they highlight the usefulness of the $^{43}Ca/^{48}Ca$ ratio as a preliminary screen of data quality. Disregarding this small portion, the Mg/Ca data delineate a profile that is approximately symmetrical about the mid-line in terms of the magnitude and spacing of the peaks (cf. Lee et al., 2004). At the edges of the valve, 0–6 mm and 11–16 mm, which grew when the brachiopod was older, Mg/Ca displays narrow peaks reaching ~-13 mmol/mol and broader minima of ~5 mmol/mol. In the centre of the valve, 6–9 mm, which grew when the brachiopod was younger, values are higher and more scattered between ~7–21 mmol/mol. The Mg/Ca variations of this transverse profile (1D) have similar peak-to-trough magnitudes (6–12 mmol/mol) and similar absolute maxima and minima (arrowed) as the data from the adult part of the ontogenetic profile from the corresponding ventral valve (Fig. 4, 1V, unshaded).

There is a good overall similarity between the $\delta^{18}O$ and averaged Mg/Ca profiles of valve 1D, with higher Mg/Ca and lighter $\delta^{18}O$ in the centre of the valve. Maximum and minimum $\delta^{18}O$ values of valve 1D (2.28‰ and 1.33‰) are very similar to those recorded in valve 1 V (2.29‰ and 1.02‰). Sr/Ca data are approximately 0.5 mmol/mol higher in the centre of the transverse profile (6–9 mm) than the edges of the valve (0–6 mm and 11–16 mm) (Fig. 4, 1D).

4.4. Variation in shell chemistry between three T. retusa shells (six valves)

Profiles of laser data from the remaining transversely sectioned *T. retusa*, shells 2 and 3, are presented in Fig. 5. All four profiles are approximately symmetrical about the mid-line, with deviation resulting from the difficulty in cutting a section exactly perpendicular to the growth axis. Sr/Ca data vary by less than 0.5 mmol/mol in all valves, and the $^{43}Ca/^{48}Ca$ ratio is constant between and across all valves. Mg/Ca peak-to-trough magnitudes are closely comparable to those seen in shell 1 (Fig. 4), with the highest magnitude, 14 mmol/mol, also seen in valves 2D and 3D. Absolute maximum and minimum Mg/Ca values are consistent between both valves of the same shell, and between all valves of three individual shells (Table 3).

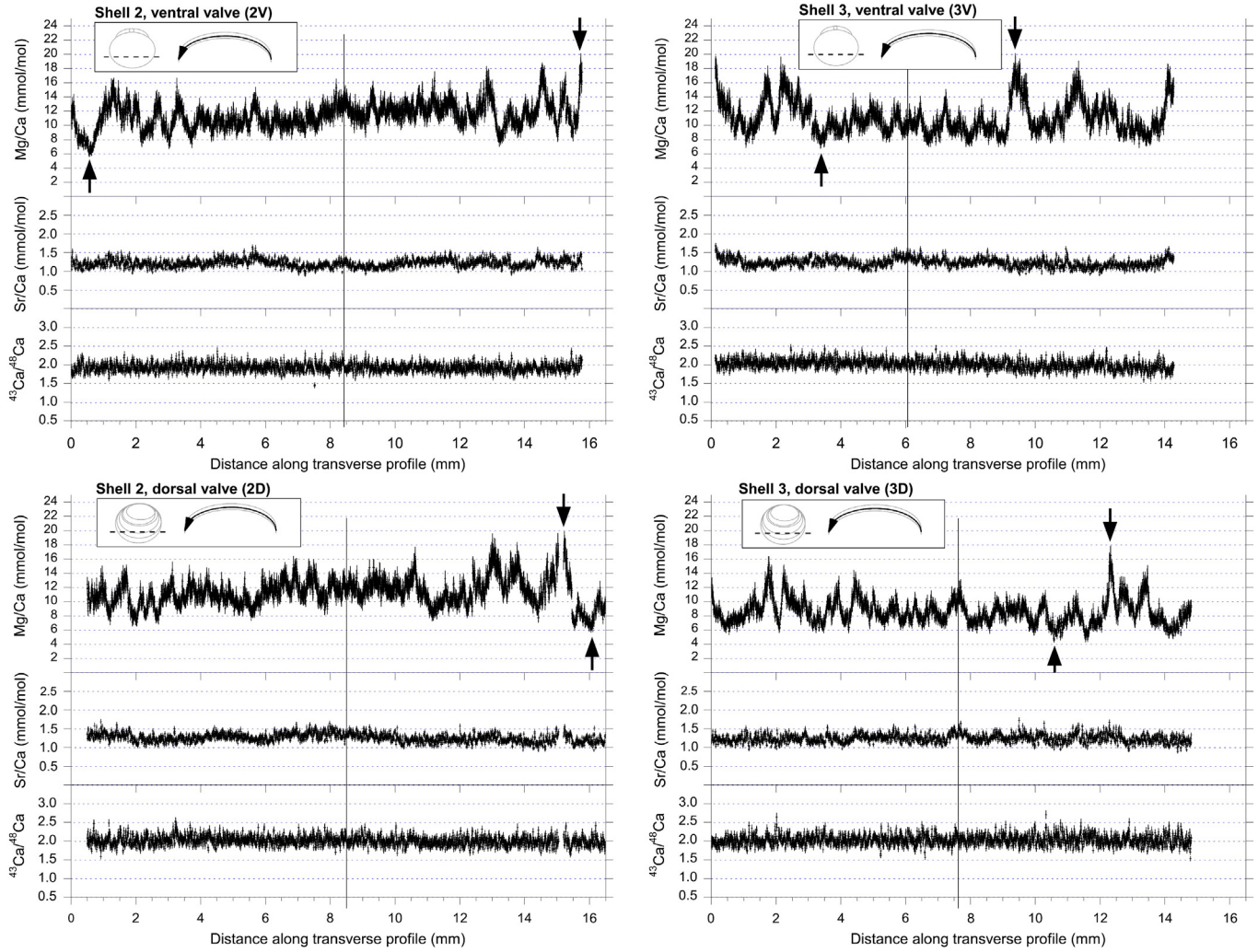

Fig. 5. Transverse profiles of laser Mg/Ca, Sr/Ca and $^{43}Ca/^{48}Ca$ intensity data from *T. retusa* shells 2 and 3. Maximum and minimum values of the Mg/Ca profiles are indicated by arrows. Vertical lines show the suggested mid-line of the valve. The *y* error bars reflect analytical uncertainty based on standards run throughout the day, ±8% RSD for Mg/Ca and ±4% RSD for Sr/Ca and $^{43}Ca/^{48}Ca$.

Table 3
Maximum and minimum Mg/Ca values and their related temperature estimates from *T. retusa* valves collected live from the same location, which has a measured temperature range of 6.5–13 °C (Curry, 1982).

Shell	Section	Valve (D = dorsal, V = ventral)	Minimum Mg/Ca (mmol/mol)	Maximum Mg/Ca (mmol/mol)	$(Mg/Ca_{Max}\text{-}Mg/Ca_{Min})/\Delta T$ (mmol/mol/°C)	Temperature estimates at location of the minimum Mg/Ca value:		Temperature estimates at location of the maximum Mg/Ca value:		Estimated seasonal temperature range (°C)
						Mg/Ca temperature using Eq. (3)	Microdrilled d18O temperature using Eq. (1)	Mg/Ca temperature using Eq. (3)	Microdrilled d18O temperature using Eq. (1)	
1	Ontogenetic	V (excluding grey shaded region on Fig. 4)	5.1	18.8	2.1	6.6	10.4	14.8	12.1	8.2
1	Transverse	D (excluding grey shaded region on Fig. 4)	5.0	19.8	2.3	6.5	8.9	15.1	11.4	8.6
2	Transverse	V	6.1	18.6	1.9	7.8		14.7		7.0
2	Transverse	D	6.2	18.4	1.9	7.9		14.7		6.8
3	Transverse	V	7.3	18.6	1.7	8.9		14.7		5.8
3	Transverse	D	4.6	16.5	1.8	6.0		14.0		8.0
Means:			**5.7 ± 0.8 (2se)**	**18.5 ± 0.9 (2se)**	**2.0 ± 0.2 (2se)**	**7.3 ± 0.8 (2se)**		**14.7 ± 0.4 (2se)**		**7.4 ± 0.8 (2se)**

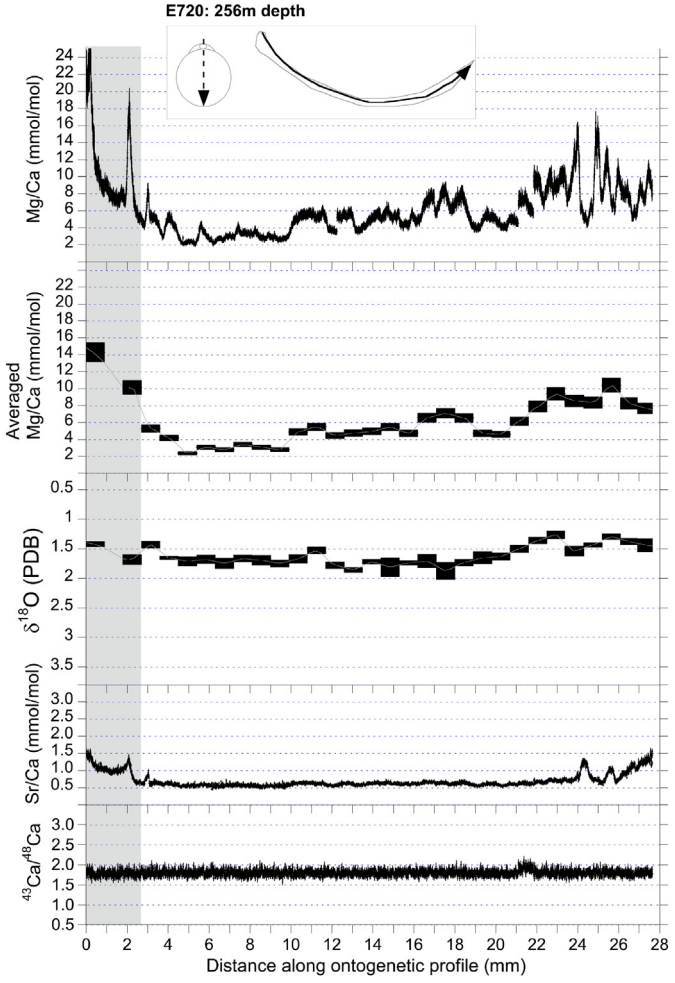

Fig. 6. Ontogenetic profile of laser Mg/Ca, Sr/Ca and $^{43}Ca/^{48}Ca$ intensity data, and microdrilled $\delta^{18}O$ data from *L. neozelanica* shell E720. 'Averaged Mg/Ca' is a plot of the laser Mg/Ca data averaged over the same distances as the trenches drilled for $\delta^{18}O$ analysis. Grey shading denotes where $\delta^{18}O$ and averaged Mg/Ca do not co-vary. For laser data, *y* error bars reflect analytical uncertainty based on standards run throughout the day (±8% RSD for Mg/Ca, and ±4% RSD for Sr/Ca and $^{43}Ca/^{48}Ca$). For $\delta^{18}O$, the *y* error bars represent ±1 SD of the individual measurements. (For interpretation of the references to colour in this figure, the reader is referred to the web version of this article.)

4.5. Geochemical variability along an ontogenetic section of *L. neozelanica*

Like the *T. retusa* data, the *L. neozelanica* ontogenetic section (valve E720) has its highest Mg/Ca values (up to 25 mmol/mol) in the most juvenile (posterior) part (0–2.5 mm, shaded grey) (Fig. 6). The remainder of the valve displays Mg/Ca variations with peak-to-trough magnitude between 3 and 12 mmol/mol, on spatial scales of ~1 mm. As observed for *T. retusa*, Mg/Ca and $\delta^{18}O$ do not co-vary in the juvenile portion of the ontogenetic section. However, the $\delta^{18}O$ and averaged Mg/Ca profiles of this *L. neozelanica* shell show a high degree of co-variation from ~2.5 mm onwards. $\delta^{18}O$ ranges from 1.3 to 1.9 ‰. The largest Sr/Ca variations seen in the adult part of the valve are ~0.7 mmol/mol in magnitude and coincide with large Mg/Ca variations (at ~24–26 mm).

The maximum and minimum and peak-to-trough amplitudes of the Mg/Ca variations seen in the adult calcite are similar to those seen in the transverse section of this shell (Fig. 7, E720).

4.6. *L. neozelanica* from a modern water depth transect

Four *L. neozelanica* shells from the New Zealand water depth transect (168 m–1488 m) were sectioned transversely (Fig. 7). With increasing

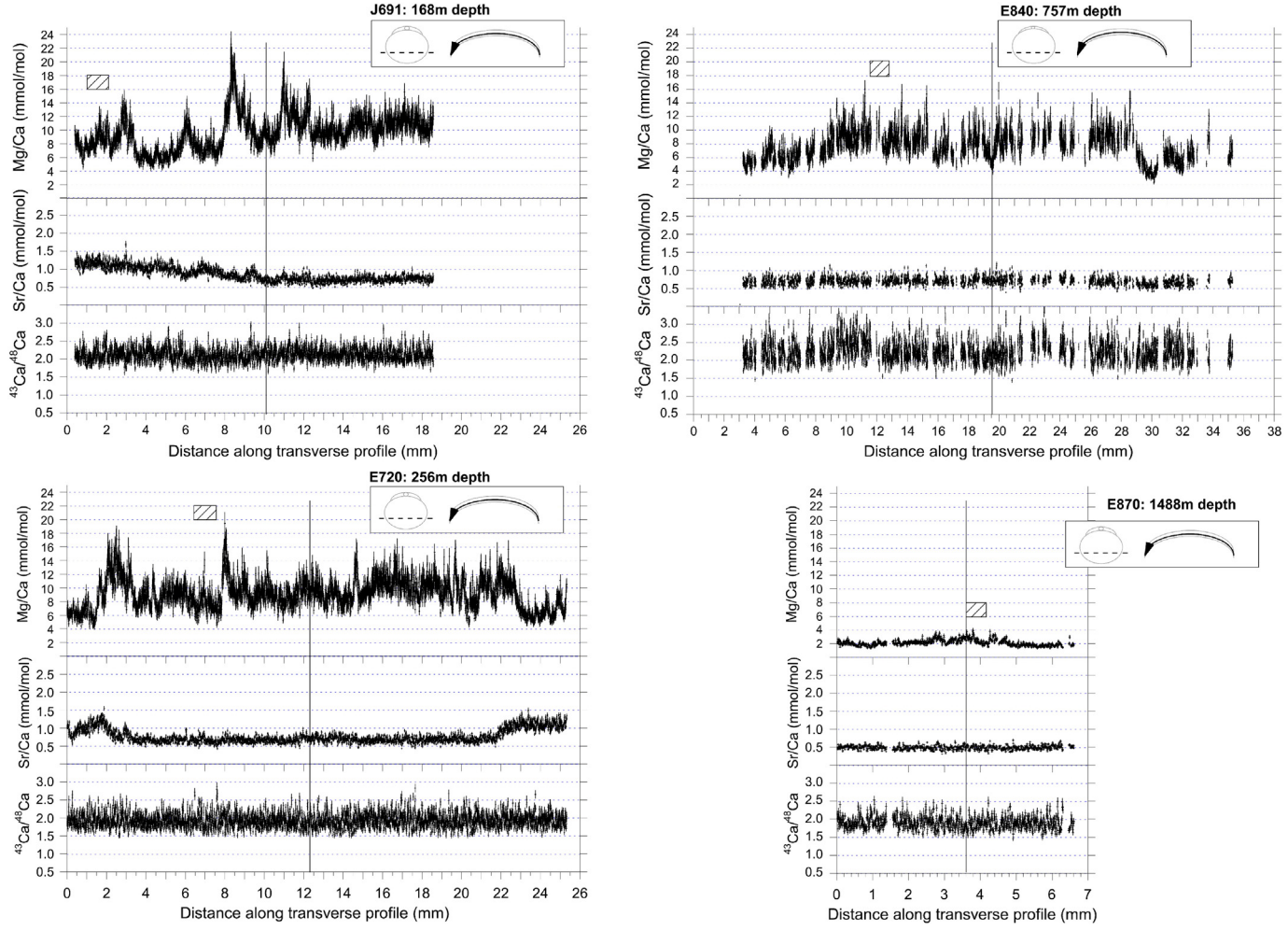

Fig. 7. Transverse profiles of laser Mg/Ca, Sr/Ca and $^{43}Ca/^{48}Ca$ intensity data from four *L. neozelanica* shells recovered from different depths. Hatched boxes indicate the location of microdrill sampling for $\delta^{18}O$ analysis. Vertical lines show the suggested mid-line of the valve. The *y* error bars reflect analytical uncertainty based on standards run throughout the day, ±8% RSD for Mg/Ca and ±4% RSD for Sr/Ca and $^{43}Ca/^{48}Ca$.

water depth of recovery, the valve profiles show a reduction in the mean Mg/Ca, as well as reduced Mg/Ca peak-to-trough amplitudes (Fig. 7, Table 4). Intra-shell Mg/Ca variation is barely discernible in valve E870, which was recovered from 1488 m water depth. The largest variation in Sr/Ca seen in these profiles is around 0.5 mmol/mol, occurring in the two valves from the shallowest depth, and the mean value of Sr/Ca decreases with increasing depth. $^{43}Ca/^{48}Ca$ profiles show no significant variation but have a larger degree of scatter in valve E840 (the valve which had the most data removed through screening for contamination by borings, as described in Section 3.3). Measurements of $\delta^{18}O$ using powder drilled from the hatched regions on Fig. 7 become heavier with increasing depth (Table 4).

5. Discussion

5.1. Elevated Mg/Ca in posterior regions of valves

In ontogenetic sections, the posterior regions of both *T. retusa* and *L. neozelanica* have strongly elevated Mg/Ca compared to the rest of the valves (Figs. 4 and 6). These are likely caused by the crystallographic

Table 4
Mg/Ca signals, $\delta^{18}O$ measurements and their related temperature estimates from *L. neozelanica* valves from four different depths.

Valve	Depth of recovery (m)	$\delta^{18}O$ (‰VPBD)	$\delta^{18}O$ temperature from Eq. (1) (°C)	Min. Mg/Ca (mmol/mol)	Max. Mg/Ca (mmol/mol)	Approx min. temperature from Mg/Ca (Eq. (4)) (°C)	Approx max. temperature from Mg/Ca (Eq. (4)) (°C)	Temperature from nearest CTD cast (°C)
J691	168	1.31 ± 0.07	13.59	~4	~24	10.5	19.5	14.6
E720 Ontogenetic section	256							
'Coldest'		1.88 ± 0.15	11.2	~2		7.0		
'Warmest'		1.26 ± 0.07	13.51		~17		17.7	13.4
E720 transverse section	256	1.64 ± 0.04	12.08	~4	~20	10.5	18.5	13.4
E840 transported downslope?	757	1.68 ± 0.03	11.01	~3	~17	9.1	17.7	7.2
E870 transported downslope?	1488	2.93 ± 0.05	6.62	~2	~4	7.0	10.5	3.2

orientation effect as observed in *T. retusa* by Perez-Huerta et al. (2011); in the posterior region where the *c*-axes of calcite crystals are randomly oriented, high and variable Mg/Ca values were reported. The remainder of the valve's secondary layer calcite, where regular fibres have *c*-axes perpendicular to the inner shell margin, yielded lower and less scattered Mg/Ca values (ibid.). This feature could possibly be a result of very fast shell growth in young brachiopods (Buening and Carlson, 1992) and is consistent with a growth band study showing that *T. retusa* are immature and fast growing up to 3 years of age (Curry, 1982). It follows that the most reliable portion of brachiopod secondary layer calcite to use for reconstructing seasonality comes from the older parts of the shell (Buening and Carlson, 1992, Perez-Huerta et al., 2011). Chemical profiles obtained from such regions of fossil brachiopod shells can be successfully interpreted as recording seasonal changes in palaeoenvironment (Mii and Grossman, 1994; Grossman et al., 1996; Powell et al., 2009).

5.2. Do brachiopod intra-shell Mg/Ca variations reflect temperature?

All of the *T. retusa* shells selected for this study experienced the same environmental conditions as they were collected alive simultaneously from one locality. Each transverse section was cut at a similar shell-age, about two-thirds of the distance from the posterior margin to avoid the crystallographic effects mentioned above. The inter-shell maximum and minimum Mg/Ca values from each profile are consistent, and average 18.5 ± 0.9 mmol/mol and 5.7 ± 0.8 mmol/mol, respectively (Table 3). The annual temperature range at the sample site is 6.5 °C. Therefore, if the intra-shell Mg/Ca variations are assumed to be a direct result of this seasonal temperature range, these data suggest a Mg/Ca–temperature sensitivity of 2.0 mmol/mol/°C (Table 3). We note that the shape of the Mg/Ca cycles in the adult portion of the *T. retusa* ontogenetic Section (Fig. 4, ~7.5 mm onwards) is saw-toothed with a steeper increase than decrease. This suggests that the brachiopod grew slowly in the winter/spring and faster in the summer/autumn. This is consistent with observations of *T. retusa* growth lines by Curry (1982), which suggest that two-thirds of the annual growth occurs in the 6 months of summer/autumn with one third of the annual growth occurring in the 6 months of winter/spring. However, different minima are seen in different years in the ontogenetic profile (Fig. 4), suggesting there was no minimum temperature at which growth shut down, which would otherwise bias our calculated Mg/Ca–temperature sensitivity. Our assumption that intra-shell brachiopod shell Mg/Ca variations reflect seasonal temperature variations can be tested using intra-shell $\delta^{18}O$ data to provide an independent measure of the temperature variation recorded within valves.

Our *T. retusa* $\delta^{18}O$ values are similar to previously published data from this species from the Firth of Lorne (1.0–2.5‰ Parkinson et al., 2005), which is also the range of expected equilibrium values for this seawater (ibid.). There is no significant annual salinity variation at this locality (Grantham, 1983; Grantham et al., 1983a, 1983b), so we interpret valve $\delta^{18}O$ data solely in terms of seawater temperature. When compared on similar spatial scales of sampling, the close co-variation of $\delta^{18}O$ and averaged Mg/Ca in the adult portions of the valve (non-shaded region in Fig. 4) support a temperature control on Mg/Ca. Using a $\delta^{18}O_{seawater}$ value of 0.06‰ VSMOW for this locality (Parkinson et al., 2005), we use the following equation to convert $\delta^{18}O$ to temperature.

$$T = 16.89 - 4.18\left(\delta^{18}O_{calcite} - \delta^{18}O_{seawater}\right) + 0.18\left(\delta^{18}O_{calcite} - \delta^{18}O_{seawater}\right)^2 \quad (1)$$

This equation is based upon the thorough delineation of the relationship between $\delta^{18}O$ and seawater temperature in modern brachiopod calcite recently provided by Brand et al. (2013); it is a second-order polynomial fit to data from their supplementary data Table S2. Unlike Brand et al. (2013), we chose not to include a correction for the effect of Mg on $\delta^{18}O$, as this is derived from a study of synthetic magnesian calcite, where it is required for Mg/Ca values above 100 mmol/mol (Jiménez-López et al., 2004). Our $\delta^{18}O$-based temperatures range from ~8.5 to 13 °C. These values do not encompass the coldest measured seawater temperatures (6.5 °C), likely because the calcite was drilled from trenches, and the brachiopods grow more slowly in the winter months. 'Averaged Mg/Ca' from the region of the microdrill trenches (black boxes in Fig. 4) are plotted versus their corresponding $\delta^{18}O$ temperatures on Fig. 8 (open triangles). Owing to the reduced spatial sampling resolution of this technique, the data lie between the points representing laser ablation Mg/Ca maxima and minima and *in situ* measured seawater temperatures. These two end members defined by measured seawater

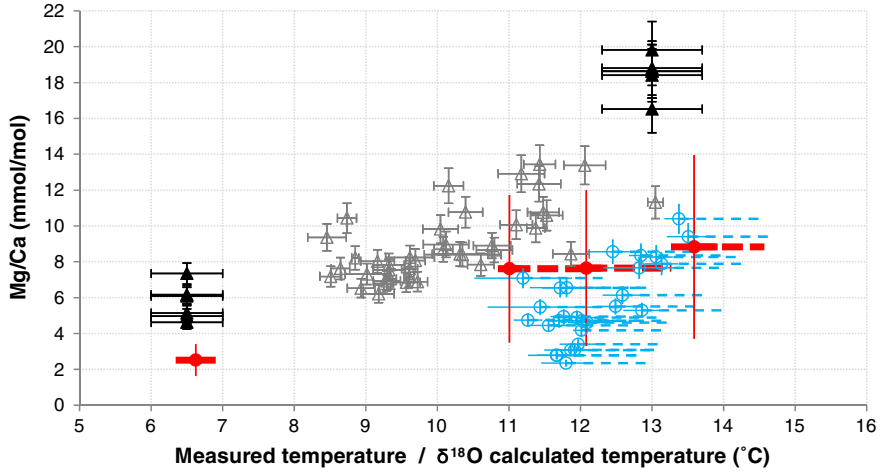

Fig. 8. Mg/Ca–temperature relationships in *T. retusa* and *L. neozelanica*. Filled triangles (*T. retusa*) plot maximum and minimum Mg/Ca values from the laser profiles of shells 1 to 3 (Figs. 4 and 5, Table 3) versus measured seawater temperature. The *x* error bars indicate the possible error in measured seawater temperature by showing the difference between seawater temperatures at depth measured in CTD casts from two subsequent summers and winters, ±0.5 °C (Grantham, 1983; Grantham et al., 1983a, 1983b). Open triangles (*T. retusa*) plot 'Averaged Mg/Ca' from Fig. 4 versus their corresponding $\delta^{18}O$ temperatures (calculated as described in Section 5.2) for the ontogenetic and transverse sections of shell 1. Closed circles (*L. neozelanica*) plot averaged laser Mg/Ca from the same region of the valve as the δ18O sampling (hatched on Fig. 7) versus the corresponding $\delta^{18}O$ temperature (calculated as described in Section 5.2) for valves from different depths. The *y* error bars show ±2 SD of the Mg/Ca data from the laser profiles of each valve (Fig. 7). Open circles (*L. neozelanica*) plot 'Averaged Mg/Ca' versus their corresponding $\delta^{18}O$ temperatures (as described in Section 5.2) for the ontogenetic section of shell E720 (Fig. 6). Unless otherwise noted, all other *x* error bars come from the substitution of ±1 SD of the $\delta^{18}O$ measurement into the temperature calculation (Eq. (1)) and all other *y* error bars reflect the analytical uncertainty in Mg/Ca based on standards run throughout the day, ±8% RSD.

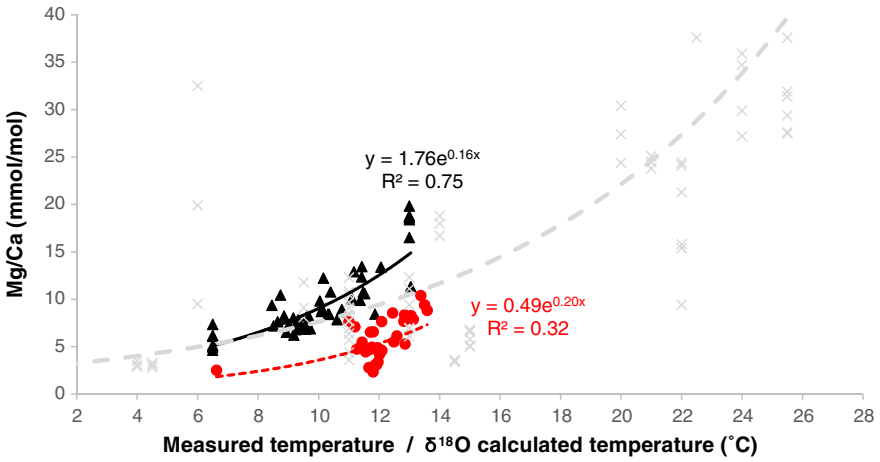

Fig. 9. Exponential curve fits for all *T. retusa* data (triangles) and all *L. neozelanica* data (circles) from Fig. 8, compared to an exponential fit through the data of Brand et al. (2013) (crosses—obtained from drilled or crushed and powdered valves from multiple species from worldwide localities. This fit includes data from >40 mmol/mol which are included in the supplementary files).

temperatures lie within the 95% confidence intervals of an exponential fit to the data defined by $\delta^{18}O$ temperatures (Eq. (2)).

$$Mg/Ca = 2.35 \pm 0.46\, e^{(0.13\pm0.04)T} \quad (2)$$

This agreement between the two approaches suggests that in the secondary layer calcite of *T. retusa*, Mg/Ca is a faithful recorder of seawater temperature. Combining the data from the two methods defines a Mg/Ca–temperature relationship (Fig. 9), which can be approximated by an exponential fit with an R^2 value of = 0.75 (Eq. (3)).

$$Mg/Ca = 1.76 \pm 0.27 e^{\left(0.16^{\pm}0.03\right)}\mathrm{T}(\text{errors are 95\% confidence intervals}) \quad (3)$$

A similar Mg/Ca–temperature relationship is also seen within intra-shell $\delta^{18}O$ and Mg/Ca data from the ontogenetic section of *L. neozelanica* shell E720. Laser ablation Mg/Ca data were averaged over the $\delta^{18}O$ sampling trench and plotted versus their corresponding $\delta^{18}O$ temperatures (open circles, Fig. 8). $\delta^{18}O$-temperatures were calculated using Eq. (1), using estimates for the $\delta^{18}O$ of seawater obtained from the salinity–$\delta^{18}O$ relationship of LeGrande and Schmidt (2006), with salinity at depth taken from the closest available CTD cast (WOCE, 2002). The impact of uncertainty in $\delta^{18}O_{sw}$ on calculated temperatures is shown by the right hand *x* error bars (dashed) on Fig. 8, which denotes the range of temperatures obtained when assuming up to 500 m post-mortem downslope transport.

5.3. Brachiopod Mg/Ca and $\delta^{18}O$ from a modern water depth transect

In general, the overall trend of increasing *L. neozelanica* $\delta^{18}O$ with water depth is consistent with water column temperature profiles (Tables 1 and 4), and the measurements are broadly comparable to published data from this species in different shallow water settings off the South Island of New Zealand (1.1–1.44 ‰ for Doubtful Sound (Brand et al., 2013) and 0.7–1.7 ‰ for the Otago Shelf (Parkinson et al., 2005)). Unfortunately, it is not known whether the shells have been transported after death prior to collection. We therefore chose to use the shell $\delta^{18}O$ as the most robust means of evaluating the *in situ* temperature during the brachiopod's lifetime. Although this approach requires an assumed value for seawater $\delta^{18}O$, the variation of this parameter with water depth is less significant than temperature. To calculate temperature we used Eq. (1), in combination with the salinity–$\delta^{18}O$ relationship of LeGrande and Schmidt (2006), with salinity at depth taken from the closest available CTD cast (WOCE, 2002). We assume a maximum post-mortem downslope transport of 500 m, which translates into a $\delta^{18}O_{sw}$-related uncertainty of + 1.19 °C on our calculated temperatures (Fig. 8). Plotting averaged Mg/Ca versus calculated $\delta^{18}O$-temperature on Fig. 8 (filled circles), defines a similar Mg/Ca–temperature sensitivity to those defined by intra-shell data from both *L. neozelanica* and *T. retusa* (described in Section 5.2).

An exponential fit through all measurements from *L. neozelanica* (intra-shell and depth profile) (Fig. 9) defines the following Mg/Ca–temperature relationship:

$$Mg/Ca = 0.49 \pm 1.27\, e^{(0.2\pm0.11)T}(\text{errors are 95\% confidence intervals}) \quad (4)$$

This equation and its large error margins are strongly influenced by the scarcity of data from low temperatures, so an aim of future work on this species should be to further constrain this initial relationship. A comparison of this initial *L. neozelanica* Mg/Ca–temperature relationship to that of *T. retusa* highlights the presence of a taxonomic offset of around 5 mmol/mol (Fig. 9), which is similar to the taxonomic differences observed in fossil brachiopods by Popp et al. (1986) and Grossman et al. (1996). Further investigation of taxonomic offsets are recommended for future work.

The Mg/Ca sensitivity to temperature for both *T. retusa* and *L. neozelanica* is similar to the overall trend obtained from drilled or crushed and powdered valves from multiple species from worldwide localities (Brand et al., 2013; Fig. 9). However, the laser ablation data are less scattered, supporting its use in better defining the Mg/Ca–temperature relationship in brachiopod shell calcite.

5.4. A potential proxy for reconstructing past seasonality?

To gain an initial insight into how many fossil valves might need to be studied to obtain meaningful estimates of seasonality for the geological past, we treated the six *T. retusa* valves as if they were fossil unknowns. For the adult portions of each valve, deemed unaffected by the crystallographic effect, we converted the difference between maximum and minimum Mg/Ca into a difference between maximum and minimum temperature (seasonality) using Eq. (3). This yields an estimate of the seasonal temperature range (7.4 °C) with a confidence in the mean of ±0.8 °C (2se, $n = 6$) (Table 3). Although this level of precision reflects the ideal situation of at least six pristinely preserved fossil valves of identical age, it is small enough to encourage development of the proxy.

6. Conclusions

Laser ablation sampling is an ideal means of identifying the full amplitude of brachiopod intra-shell trace metal variations. Our results strongly support a temperature (seasonality) control on brachiopod intra-shell Mg/Ca cycles in the adult portion of the brachiopod shell. Laser ablation sampling of brachiopod shells also defines the shape of seasonal cycles in Mg/Ca, allowing assessment of whether the full seasonal temperature range is captured in a shell. We also compared two different profile-sectioning techniques. Sectioning brachiopod shells longitudinally has the advantage of capturing an increased number of seasonal cycles, which may be useful for estimating past seasonality, although care must be taken to avoid sampling the juvenile material in the posterior part of the shell. Sectioning brachiopods transversely, about two-thirds of the shell length from the posterior margin avoids this problem. Furthermore, this traverse produces an approximately symmetrical seasonal signal either side of the axis of symmetry, which could be a useful constraint on assessing the robustness of seasonal Mg/Ca cycles observed in fossil shells that may have undergone more diagenetic processes.

Our estimated Mg/Ca–temperature sensitivity is higher than that for inorganic calcite, but similar to other biogenic calcites, suggesting a combined thermodynamic and physiological control on the uptake of Mg into brachiopod shell calcite. The sensitivity is similar for both *T. retusa* and *L. neozelanica* and is higher than the linear Mg/Ca–temperature calibrations for the calcite layers of the bivalves *Mytilus trossulus* (Klein et al., 1996), and *Mytilus edulis* (Vander Putten et al., 2000) which has previously been applied to fossil brachiopod Mg/Ca data (Powell et al., 2009).

In summary, laser ablation Mg/Ca profiles of brachiopod calcite have great potential as a palaeothermometer, capturing both secular variations in bottom water temperatures and also past changes in the degree of seasonality.

Supplementary data to this article can be found online at http://dx.doi.org/10.1016/j.chemgeo.2015.01.009.

Acknowledgements

Dr. Steve Chiswell, Dr. Kareen Schnabel and Sadie Mills from the National Institute of Water and Atmospheric Research (NIWA) Invertebrate Collection, New Zealand, are thanked for providing *L. neozelanica* valves and assistance with CTD data. Drs. Julia Becker and Sandra Nederbragt are thanked for their assistance with stable isotope analyses, and Amanda Valentine-Baars of the National Museum Wales is thanked for her advice on sectioning valves. The manuscript was improved by the careful comments of two anonymous reviewers. This work was funded by a NERC Open CASE award NE/H018018/1 to Cardiff University and Amgueddfa Cymru, National Museum Wales (CHL and TRB); the studentship was awarded to SB.

References

Auclair, A.C., Joachimski, M.M., Lécuyer, C., 2003. Deciphering kinetic, metabolic and environmental controls on stable isotope fractionations between seawater and the shell of *Terebratalia transversa* (Brachiopoda). Chem. Geol. 202 (1), 59–78.

Barker, S., Greaves, M., Elderfield, H., 2003. A study of cleaning procedures used for foraminiferal Mg/Ca paleothermometry. Geochem. Geophys. Geosyst. 4.

Brand, U., Veizer, J., 1980. Chemical diagenesis of a multicomponent carbonate system.1. Trace-elements. J. Sediment. Petrol. 50, 1219–1236.

Brand, U., 2004. Carbon, oxygen and strontium isotopes in Paleozoic carbonate components: an evaluation of original seawater-chemistry proxies. Chem. Geol. 204 (1), 23–44.

Brand, U., Azmy, K., Bitner, M.A., Logan, A., Zuschin, M., Came, R., Ruggiero, E., 2013. Oxygen isotopes and $MgCO_3$ in brachiopod calcite and a new paleotemperature equation. Chem. Geol. 359, 23–31.

Brand, U., Came, R.E., Affek, H., Azmy, K., Mooi, R., Layton, K., 2014. Climate-forced change in Hudson Bay seawater composition and temperature, Arctic Canada. Chem. Geol. 388, 78–86.

Buening, N., Carlson, S.J., 1992. Geochemical investigation of growth in selected recent articulate brachiopods. Lethaia 25, 331–345.

Chivas, A.R., Dedeckker, P., Shelley, J.M.G., 1986. Magnesium content of nonmarine ostracod shells—a new paleosalinometer and paleothermometer. Palaeogeogr. Palaeoclimatol. Palaeoecol. 54, 43–61.

Curry, G.B., 1982. Ecology and population-structure of the recent brachiopod *T. retusa* from Scotland. Palaeontology 25, 227–246.

Cusack, M., Perez-Huerta, A., Janousch, M., Finch, A.A., 2008. Magnesium in the lattice of calcite-shelled brachiopods. Chem. Geol. 257, 59–64.

Dwyer, G.S., Cronin, T.M., Baker, P.A., Raymo, M.E., Buzas, J.S., Correge, T., 1995. North-Atlantic deep-water temperature-change during Late Pliocene and Late Quaternary climate cycles. Science 270, 1347–1351.

Grantham, B., 1983. Firth of Lorne Study, Reports 1 and 2. Scottish Marine Biological Association, Oban.

Grantham, B., Boyd, D., Gowen, R., Lewis, J., Weeks, A., 1983a. Firth of Lorne Study, Report 3. Scottish Marine Biological Association, Oban.

Grantham, B., Chadwick, A., Shaw, J., 1983b. Firth of Lorne Study, Report 4. Scottish Marine Biological Association, Oban.

Grossman, E.L., Mii, H.S., Zhang, C., Yancey, T.E., 1996. Chemical variation in Pennsylvanian brachiopod shells; diagenetic, taxonomic, microstructural, and seasonal effects. J. Sediment. Res. 66 (5), 1011–1022.

Jiménez-López, C., Romanek, C.S., Huertas, F.J., Ohmoto, H., Caballero, E., 2004. Oxygen isotope fractionation in synthetic magnesian calcite. Geochim. Cosmochim. Acta 68 (16), 3367–3377.

Klein, R.T., Lohmann, K.C., Thayer, C.W., 1996. Bivalve skeletons record sea-surface temperature and δ18O via Mg/Ca and 18O/16O ratios. Geology 24 (5), 415–418.

Lee, X.Q., Hu, R.Z., Brand, U., Zhou, H., Liu, X.M., Yuan, H.L., Yan, C.L., Cheng, H.G., 2004. Ontogenetic trace element distribution in brachiopod shells: an indicator of original seawater chemistry. Chem. Geol. 209, 49–65.

LeGrande, A.N., Schmidt, G.A., 2006. Global gridded data set of the oxygen isotopic composition in seawater. Geophys. Res. Lett. 33. http://dx.doi.org/10.1029/2006GL026011 L12604.

Linnaeus [Linné], C., 1758. Systema Naturae. 10th ed. sive Regna tria Naturae systematicae proposita per Classes, Ordines, Genera et Species vol. 1 (Holmiae. Stockholm. 823 p).

Logan, A., 2007. Geographic distribution of extant articulated brachiopods. In: Selden, P. (Ed.), Treatise on Invertebrate Paleontology Brachiopoda (Part H6) Revised. Geological Society of America.

Lowenstam, H.A., 1961. Mineralogy, O-18/O-16 ratios, and strontium and magnesium contents of recent and fossil brachiopods and their bearing on the history of the oceans. J. Geol. 69, 241–260.

Mii, H.S., Grossman, E.L., 1994. Late Pennsylvanian seasonality reflected in the 18O and elemental composition of a brachiopod shell. Geology 22 (7), 661–664.

Nürnberg, D., Bijma, J., Hemleben, C., 1996. Assessing the reliability of magnesium in foraminiferal calcite as a proxy for water mass temperatures. Geochim. Cosmochim. Acta 60, 2483-2483.

Parkinson, D., Curry, G.B., Cusack, M., Fallick, A.E., 2005. Shell structure, patterns and trends of oxygen and carbon stable isotopes in modern brachiopod shells. Chem. Geol. 219, 193–235.

Pearce, N.J.G., Perkins, W.T., Westgate, J.A., Gorton, M.P., Jackson, S.E., Neal, C.R., Chenery, S.P., 1997. A compilation of new and published major and trace element data for NIST SRM 610 and NIST SRM 612 glass reference materials. Geostand. Newslett. 21, 115–144.

Perez-Huerta, A., Cusack, M., Jeffries, T.E., Williams, C.T., 2008. High resolution distribution of magnesium and strontium and the evaluation of Mg/Ca thermometry in recent brachiopod shells. Chem. Geol. 247, 229–241.

Perez-Huerta, A., Cusack, M., Dalbeck, P., 2011. Crystallographic contribution to the vital effect in biogenic carbonates Mg/Ca thermometry. Trans. R. Soc. Edinb. Earth Environ. Sci. 102, 35–41.

Pérez-Huerta, A., Aldridge, A.E., Endo, K., Jeffries, T.E., 2014. Brachiopod shell spiral deviations (SSD): Implications for trace element proxies. Chem. Geol. 374, 13–24.

Popp, B.N., Anderson, T.F., Sandberg, P.A., 1986. Brachiopods as indicators of original isotopic compositions in some Paleozoic limestones. Geol. Soc. Am. Bull. 97 (10), 1262–1269.

Powell, M.G., Schöne, B.R., Jacob, D.E., 2009. Tropical marine climate during the late Paleozoic ice age using trace element analyses of brachiopods. Palaeogeogr. Palaeoclimatol. Palaeoecol. 280 (1), 143–149.

Rosenthal, Y., Boyle, E.A., Slowey, N., 1997. Temperature control on the incorporation of magnesium, strontium, fluorine, and cadmium into benthic foraminiferal shells from Little Bahama Bank: prospects for thermocline paleoceanography. Geochim. Cosmochim. Acta 61, 3633–3643.

Thomson, 1918. Brachiopoda. Australian Antarctic Expedition 1911–1914. Scientific Reports, Series C vol IV, part 3 (75 pp. 4 pls).

Vander Putten, E., Dehairs, F., Keppens, E., Baeyens, W., 2000. High resolution distribution of trace elements in the calcite shell layer of modern *Mytilus edulis*: environmental and biological controls. Geochim. Cosmochim. Acta 64, 997–1011.

Veizer, J., Fritz, P., Jones, B., 1986. Geochemistry of brachiopods: oxygen and carbon isotopic records of Paleozoic oceans. Geochim. Cosmochim. Acta 50, 1679–1696.

Williams, A., Cusack, M., 2007. Chemicostructural diveristy of the Brachiopod shell. In: Selden, P. (Ed.), Treatise on Invertebrate Paleontology Brachiopoda (Part H6) Revised. Geological Society of America.

Williams, A., Carlson, S.J., Brunton, C.H.C., Holmer, L.E., Popov, L., 1996. A supra-ordinal classification of the Brachiopoda. Philos. Trans. R. Soc. B 351, 1171–1193.

WOCE Data Products Committee, 2002. World Ocean Circulation Experiment Global Data, Version 3.0. WOCE Report No. 180/02, Southampton, UK. WOCE International Project Office.

Yamamoto, K., Asami, R., Iryu, Y., 2010a. Carbon and oxygen isotopic compositions of modern brachiopod shells from a warm-temperate shelf environment, Sagami Bay, central Japan. Palaeogeogr. Palaeoclimatol. Palaeoecol. 291, 348–359.
Yamamoto, K., Asami, R., Iryu, Y., 2010b. Within-shell variations in carbon and oxygen isotope compositions of two modern brachiopods from a subtropical shelf environment off Amami-o-shima, southwestern Japan. Geochem. Geophys. Geosyst. 11.
Yamamoto, K., Asami, R., Iryu, Y., 2011. Brachiopod taxa and shell portions reliably recording past ocean environments: toward establishing a robust paleoceanographic proxy. Geophys. Res. Lett. 38.
Zhang, Z., Robson, S.P., Emig, C., Shu, D., 2008. Early Cambrian radiation of brachiopods: a perspective from South China. Gondwana Res. 14, 241–254.